

## S7 Predictions of *corrected m-Tau* for the Psychophysical Experiment

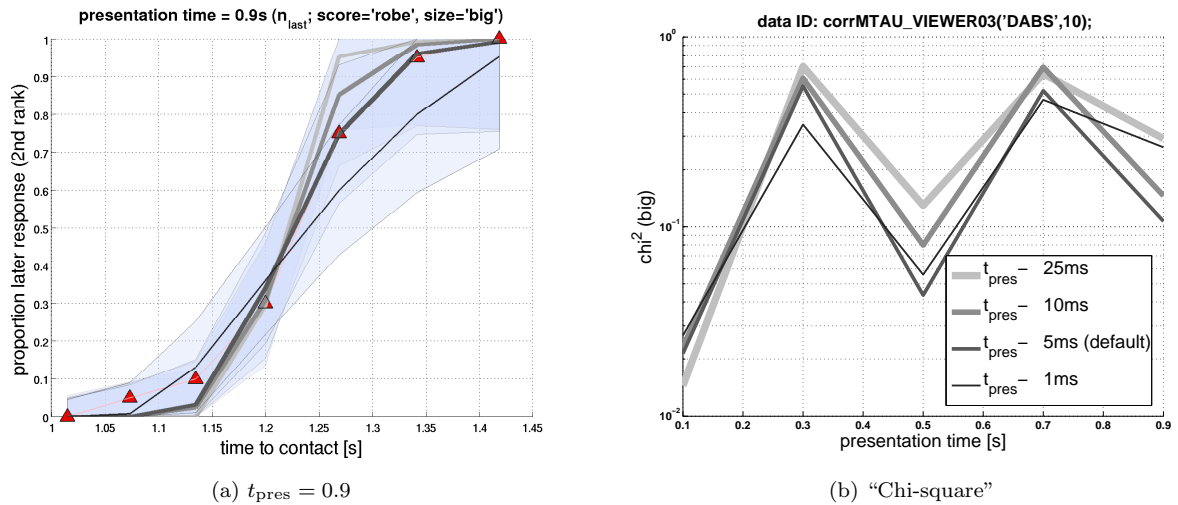


Figure S47: *Corrected m-Tau* predictions for different  $n_{last}$  (second  $E_{rob}$  rank; *big* diameter). For the simulation of our psychophysical study, we had to compute whether the *ttc*-prediction (equation 12) of the *corrected m-Tau*-model at  $t_{pres}$  was before or after  $t_{ref}$ . This *ttc*-prediction is computed according to equation (14), by averaging  $t_c(t) \approx \tau_{cm}(t) + t$  from  $t = t_{pres} - n_{last} \times 1 \text{ ms}$  to  $t = t_{pres}$ . (a) Illustration of the effect of using different averaging intervals ( $n_{last} \times 1 \text{ ms} \in \{1, 5, 10, 25 \text{ ms}\}$ ) on model predictions ( $\tau_{cm}$  parameters according to second best  $E_{rob}$  rank in Table S2 in *Text S5*). The right panel (b) shows “Chi-square” as a measure of “goodness-of-prediction” (section 15.1.1 in [1] – smaller values mean better predictions of psychophysical data). “Chi-square” is a standard-deviation-weighted root mean square error. The standard-deviations correspond to the blue-shaded areas in the left figure panel (see Methods Section). Standard deviations decrease with increasing  $t_{pres}$ , such that higher weighting is given to longer presentation times.

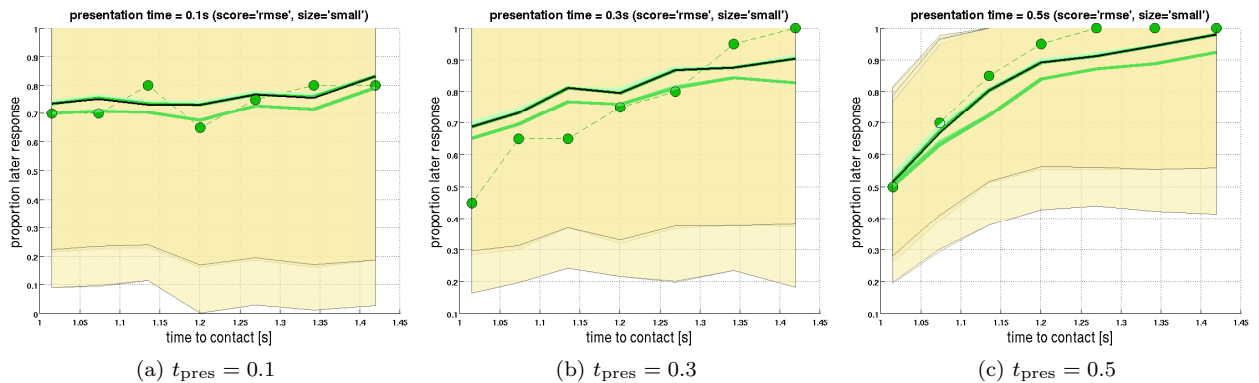


Figure S48: *Corrected m-Tau* predictions for psychophysical proportion of later response I ( $E_{rms}$  score; *small* diameter). Analogous to Figure 8 - but here parameters were optimized for the *small* diameter, according to  $E_{rms}$  scores (Table S1 in *Text S5*).

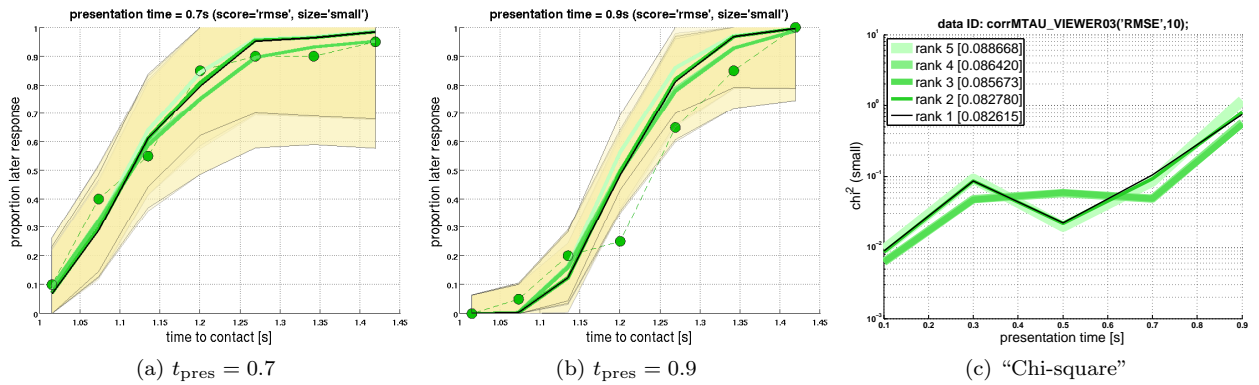


Figure S49: *Corrected m-Tau predictions II* ( $E_{rms}$  score; *small* diameter). Same as the previous figure, but for the remaining two presentation times. (c) See Figure S47b for an explanation.

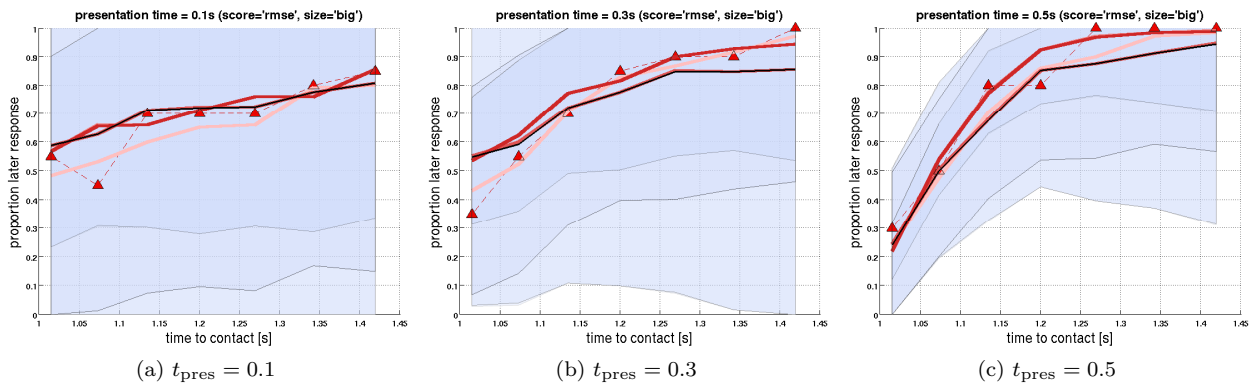


Figure S50: *Corrected m-Tau predictions I* ( $E_{rms}$  score; *BIG* diameter). Analogous to Figure 8 – but here with parameters optimized for the *big* diameter, according to  $E_{rms}$  scores (Table S2 in *Text S5*).

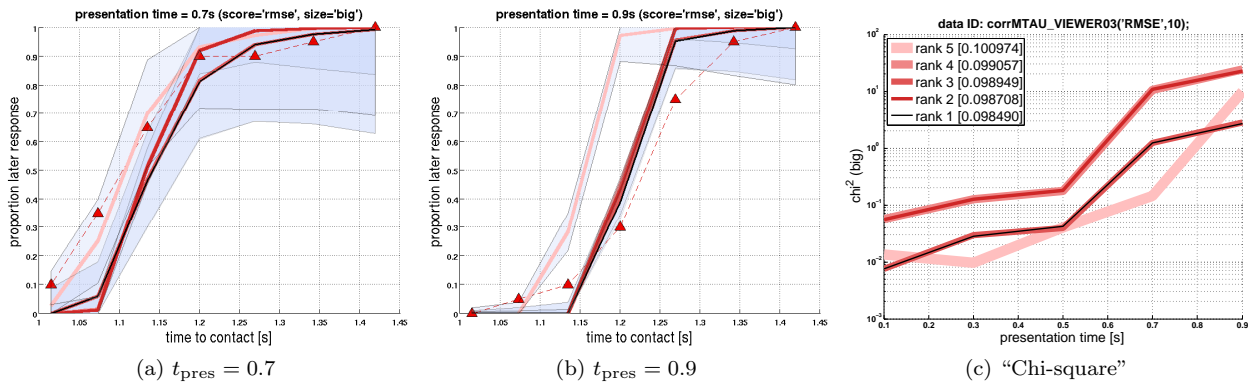


Figure S51: *Corrected m-Tau predictions II* ( $E_{rms}$  score; *BIG* diameter). Same as the previous figure, but for the remaining two presentation times. (c) See Figure S47b for an explanation.

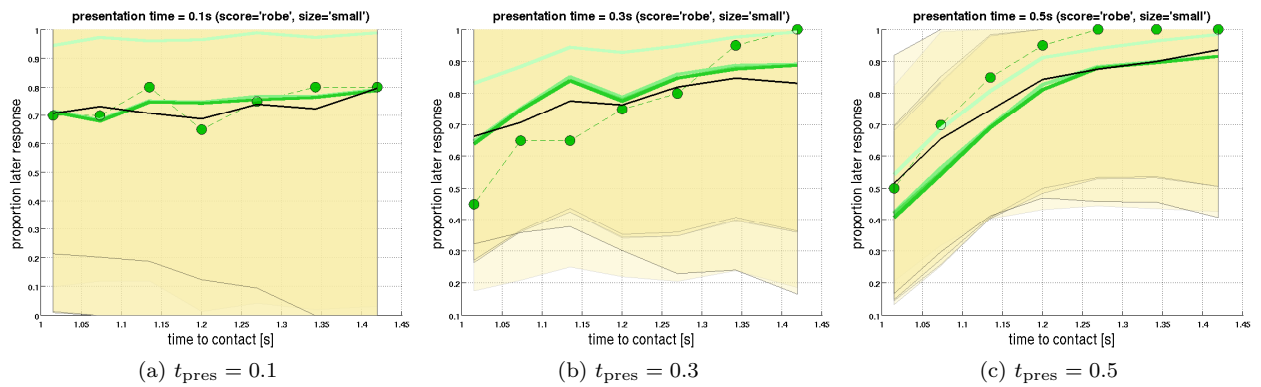


Figure S52: *Corrected m-Tau predictions I* ( $E_{\text{rob}}$  score; *small* diameter). Analogous to Figure 8 – but here  $\tau_{\text{cm}}$ -parameters were optimized for the *small* diameter, according to  $E_{\text{rob}}$  scores (Table S1 in *Text S5*).

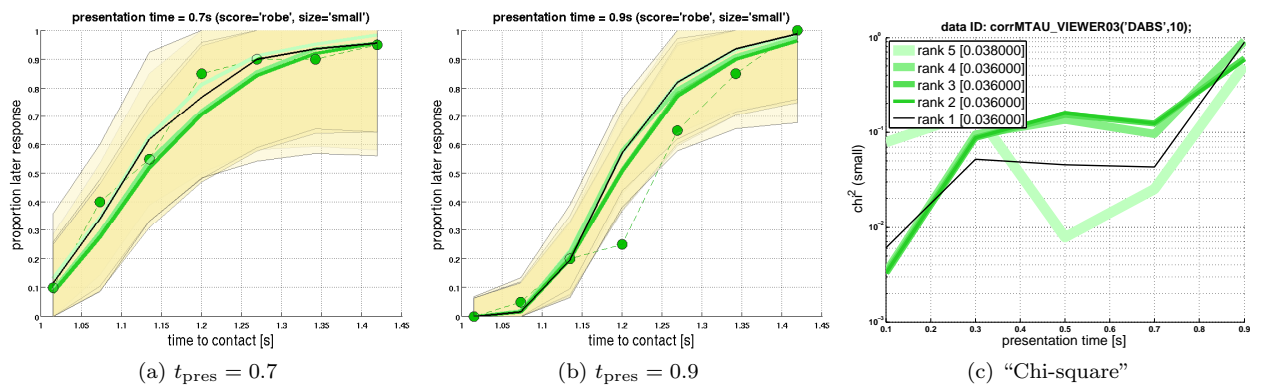


Figure S53: *Corrected m-Tau predictions II* ( $E_{\text{rob}}$  score; *small* diameter). Same as the previous figure, but for the remaining two presentation times. (c) See Figure S47b for an explanation.

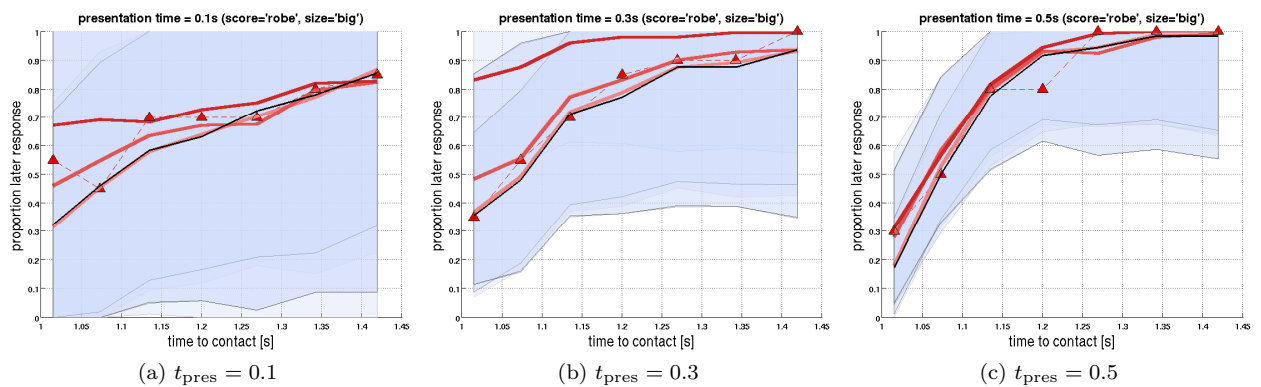


Figure S54: *Corrected m-Tau predictions I* ( $E_{\text{rob}}$  score; *BIG* diameter). Analogous to Figure 8 - but here parameters were optimized for the *big* diameter, according to  $E_{\text{rob}}$  scores (Table S2 in *Text S5*).

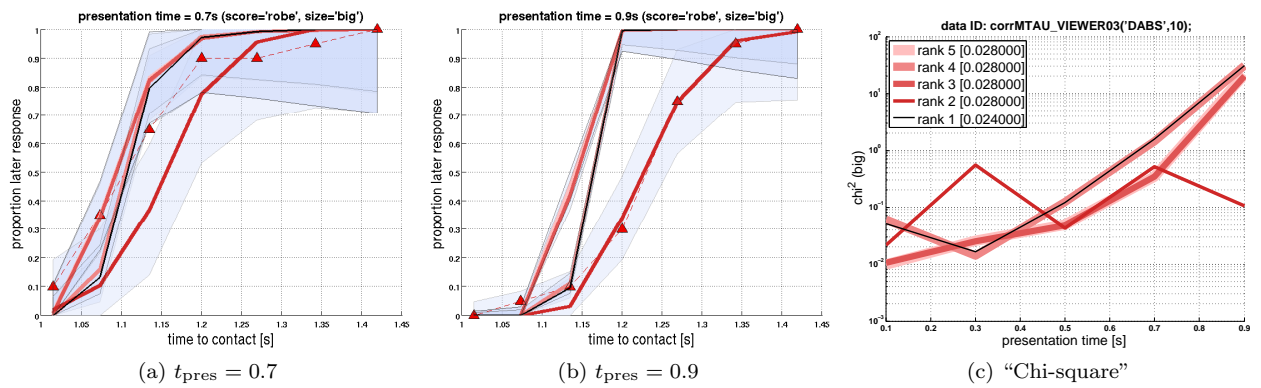


Figure S55: *Corrected m-Tau predictions II* ( $E_{rob}$  score; *BIG* diameter). Same as the previous figure, but for the remaining two presentation times. (c) See Figure S47b for an explanation.

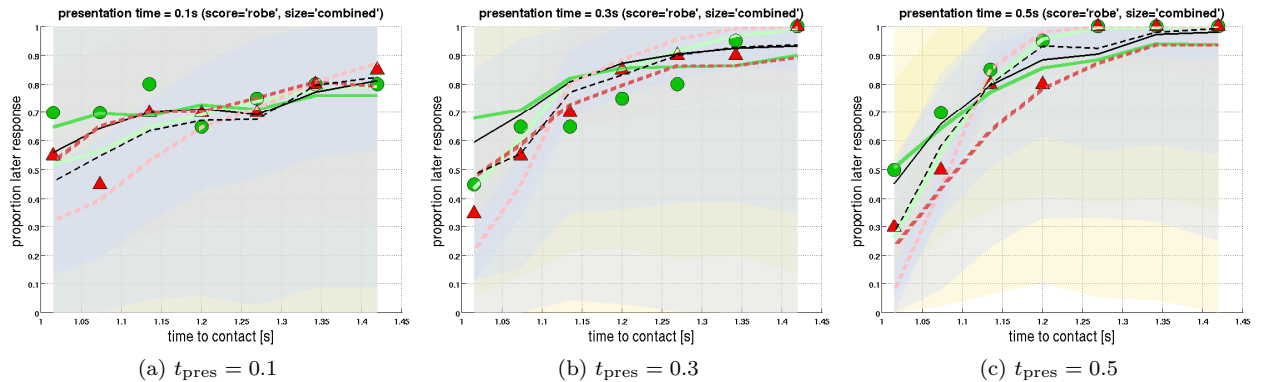


Figure S56: *Corrected m-Tau predictions I* ( $E_{rob}$  score; *combined* diameter). Analogous to Figure 8 - but here with the three best performing parameter sets according to  $E_{rob}$  scores (Table S3 in *Text S5*). Notice that the  $\tau_{cm}$ -predictions for both object diameters were computed with the same parameter set.

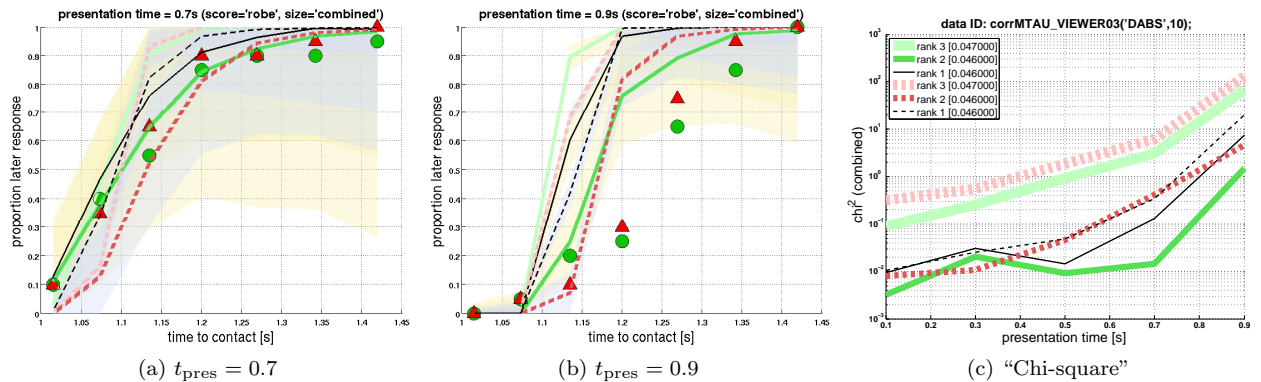


Figure S57: *Corrected m-Tau predictions II* ( $E_{rob}$  score; *combined* diameter). Same as the previous figure, but for the remaining two presentation times. (c) See Figure S47b for an explanation.

## References

1. Press H, Teukolsky S, Vetterling W, Flannery B (2007) Numerical Recipes: The Art of Scientific Computing, Third Edition. Cambridge University Press.